JOURNAL OF CATALYSIS 78, 406–418 (1982)

Reactions of *n*-Butane and Neopentane on Titania-Supported Iridium Catalysts

K. FOGER

CSIRO Division of Materials Science, Catalysis and Surface Science Laboratory, University of Melbourne, Parkville, 3052, Victoria, Australia

Received February 17, 1982; revised August 5, 1982

The reactions of *n*-butane and neopentane have been studied over titania-supported iridium catalysts of varying dispersions ($0.1 \leq D \leq 1.0$). The catalysts were characterized by electron microscopy and adsorption and temperature-programmed desorption of hydrogen. After low temperature reduction (473 K) hydrogenolysis of *n*-butane occurred in the C_2-unit mode and hydrogenolysis of neopentane in the iso-unit mode. Both reaction types are dependent on $\bar{d}_{Ir}$, and highly active sites, especially for the reaction in the iso-unit mode, are present in catalysts with $\bar{d}_{Ir} \geq 3.5$ nm. Treatment in hydrogen above 600 K caused partial reduction of titania and Ti^{3+} centers so produced interact strongly with the iridium particles (strong metal–support interaction, SMSI). Catalysts in the SMSI state are unable to adsorb hydrogen and for hydrocarbon reactions their catalytic activities fall by factors of 10^2 to 10^4. The selectivity changes which are observed may be attributed to morphological differences between SMSI and non-SMSI catalysts. Treatment in 1% oxygen in helium at 473 K followed by reduction in hydrogen at 473 K successfully destroyed the SMSI state in the case of highly dispersed Ir/TiO_2 catalysts ($\bar{d}_{Ir} \leq 1.0$ nm), but higher oxidation temperatures (673 K) are necessary to break the strong metal–support interaction in the case of less highly dispersed iridium catalysts. IrO_2 crystals are formed in oxygen at temperatures above 573 K and the catalysts undergo irreversible structural changes.

INTRODUCTION

Metals supported on refractory oxides are used as catalysts for a wide range of reactions. High surface area supports (in excess of 200 m^2/g) stabilize high metal dispersions and thus promote the most efficient use of the catalytic functions of the metal. The choice of the support material depends on the particular catalyst application and parameters such as porosity, surface area, and thermal stability must be considered. Generally supports can be classified as follows: (i) inert supports with no significant influence on adsorption or reaction properties of the metal; (ii) catalytically active supports taking part *directly* in the reactions (bifunctional systems); and (iii) supports which interact with the metal clusters and thus affect the adsorption, and reaction behavior of the catalysts indirectly. Such metal–support interactions either determine the structure of the metal clusters ("chemoepitaxial effect") as has been reported by Dalmai-Imelik *et al.* (*1*) for nickel catalysts, or, if electron transfer between the metal clusters and the substrate occurs, result in changed electronic properties of the metal particles.

Electron-deficient platinum clusters are claimed to form inside zeolite cages (*2–4*) by interaction with zeolite electron-acceptor sites. A strong dependence of reaction rate data on the electronic nature of the supports has been reported by Schwab (*5*) for the dehydrogenation of formic acid on nickel evaporated onto p- or n-type semiconductors.

A new type of metal support interaction was demonstrated by Tauster *et al.* (*6, 7*) for metals supported on transition metal oxides such as TiO_2, V_2O_5, Nb_2O_5, and Ta_2O_5 and treated in hydrogen at temperatures in excess of 700 K. The effect was named

0021-9517/82/120406-13$02.00/0

SMSI (strong metal–support interaction) and was attributed to an electron transfer from the partially reduced oxide surface to the metal clusters and the formation of "electron-rich" metal. Catalysts in the SMSI state were unable to adsorb hydrogen and carbon monoxide. In a molecular orbital study of platinum on titania, Horsley (*8*) proposed a model for the SMSI state, which is supported by binding energy shifts towards negative metal oxidation states observed by ESCA for platinum/titania (*9, 10*) and rhodium/titania (*10*) catalysts after high-temperature hydrogen treatment. Furthermore, Baker *et al.* (*11*) studied evaporated platinum particles on titania and silica by electron microscopy and observed after reduction in hydrogen at 800 K the formation of flat "pillboxes" of platinum on titania instead of the hemispherical particles obtained under those conditions on silica. This implies that catalysts in the SMSI state differ structurally and electronically from non-SMSI catalysts.

In an extensive study of silica and alumina-supported iridium (*12*), we have already established a very distinct reaction pattern for hydrocarbon conversions on iridium and proposed two types of reaction mechanisms (see Ref. *13*). Changes in the morphology and the electronic properties of the iridium particles are expected to influence the reaction behavior of those particles, and we therefore decided to extend these studies to the conversions of two characteristic hydrocarbon molecules, *n*-butane and neopentane, over titania-supported iridium catalysts reduced in hydrogen at 473 and 773 K. In addition, adsorption and temperature-programmed desorption of hydrogen was measured to assess the influence of various thermal treatments in hydrogen and oxygen on the adsorption behavior of the catalysts.

EXPERIMENTAL

Catalysts. The support materials used in this work were an 80% anatase–20% rutile mixture (Degussa P25) with a surface area of 50 $m^2 g^{-1}$, pure anatase (Tioxide) with a surface area of 120 $m^2 g^{-1}$, and pure rutile (Tioxide) with a surface area of 24 $m^2 g^{-1}$. The catalysts were prepared by impregnating those supports with chloriridic acid using the method of incipient wetness. After drying in air at 380 K the catalysts were reduced in a stream of hydrogen at 473 K for 15 hr. The metal content of the catalysts was analyzed by atomic absorption spectroscopy. The chlorine content of the catalysts was estimated from XPS data, which showed a 10-fold reduced chlorine peak after treatment with hydrogen at 473 K compared to the freshly impregnated catalyst. Thus the maximum chloride ion concentration has to be less than 0.5% even for catalysts containing 5% metal. Further characterization was carried out using transmission electron microscopy (TEM) and adsorption and temperature-programmed desorption (TPD) of hydrogen. The methods and their evaluation have been reported earlier (*12, 13*).

The catalysts were subjected to various selected treatments. High-temperature reduction was carried out in a stream of hydrogen at 773 K for 15 hr. The standard reactivation procedure after high-temperature reduction consisted of treatment in a stream of oxygen or 1% oxygen in helium (flowrate 20 $cm^3 min^{-1}$) at 473 or 673 K for 2 hr followed by reduction in flowing hydrogen at 473 K for further 2 hr.

Reaction studies. The reactions of *n*-butane and neopentane were carried out in a fixed bed reactor operating in a differential mode at low conversions. After pretreatment under selected conditions the catalysts were brought to the reaction temperature in the range 450 to 520 K in a stream of hydrogen and the reaction mixture (normally a hydrogen/hydrocarbon mixture in a molar ratio of 20 to 1) was passed through the reactor at a total pressure of 101 kPa. In this temperature range both reactions occur exclusively on the metal surface and are not influenced by support acidity and chloride ion impurities (*12*). The products were analyzed by gas chromatography using a 2-m packed column (dimethylsulfolane on fire brick) and an FID detector.

Product distributions are given in mole percentage of the reactant converted, and the reaction rates are given as turnover frequencies, N_T, evaluated according to the formula

$$N_T = \frac{2.51 \times 10^{17} \times P \times f \times \chi_{HC}}{W_c \times n_{(s)Ir}}$$

where f is the flow rate at 293 K (cm^3 s^{-1}), χ is the molar fraction of hydrocarbon in feed (0.05), P is the percentage conversion, W_c is the weight of catalyst (g), and $n_{(s)Ir}$ is iridium surface atoms per gram of catalyst (from H_2 adsorption or TEM).

RESULTS

Catalysts

The catalysts used in this work are listed in Table 1, which also contains data on mean particle sizes and numbers of surface iridium atoms, calculated from hydrogen adsorption.

Hydrogen Adsorption Data

Table 2 summarizes hydrogen adsorption values and dispersions ($D = n_{(s)Ir}/n_{(total)Ir}$) for the catalysts reduced at 473 K, after treatment in hydrogen at 773 K for 15 hr, and after subsequent oxidation treatment at 673 K for 2 hr followed by reduction in hydrogen at 473 K for 2 hr. For comparison, dispersions values obtained from TEM images are also included.

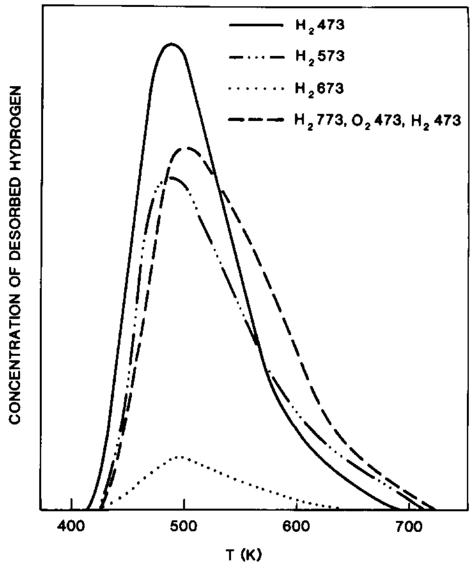

FIG. 1. TPD profiles of hydrogen from catalyst A_1 pretreated at indicated conditions.

Temperature-Programmed Desorption (TPD) of Hydrogen

The desorption profiles after adsorption of hydrogen at 298 K are shown in Figs. 1 and 2 for catalysts A_1 and A_2. After reduction at 773 K the amounts of desorbing hydrogen were below the detection limits of the apparatus in the case of both catalysts.

Reaction Data

The reaction behavior of the fresh catalysts—after reduction at $T < 520$ K—is summarized in Table 3, which lists initial product distributions, activation energies,

TABLE 1

Catalysts after Reduction at 473 K

Catalyst	Support	Metal content (%)	Mean particle size (nm) by TEM	$n_{(s)Ir}$(g cat)$^{-1}$ ($\times 10^{19}$)
A_1	P25 (Degussa)	1.0	≤1.0	3.2
A_2	P25 (Degussa)	5.0	3.5	4.8
B_1	Anatase (Tioxide)	1.1	≤1.0	3.4
C_1	Rutile (Tioxide)	0.2	≤1.0	0.6
C_2	Rutile (Tioxide)	5.0	~10.0	1.4

TABLE 2

Hydrogen Adsorption Data

Catalyst	Treatment	H_2 adsorption (molecules H_2 (g cat)$^{-1}$)	$D_{(H_2\ ads)}$	D_{TEM}
A_1	H_2 473 K	1.6×10^{19}	1.0	1.00
	H_2 773 K	Very small ($<10^{17}$)	—	1.00[a]
	H_2 773 K, O_2 673 K, H_2 473 K	0.6×10^{19}	0.38	0.35
A_2	H_2 473 K	2.4×10^{19}	0.31	0.30
	H_2 773 K	$<10^{17}$	—	0.30[a]
	H_2 773 K, O_2 673 K, H_2 473 K	2.9×10^{19}	0.38	0.35
B_1	H_2 473 K	1.7×10^{19}	1.00	1.00
	H_2 773 K	$<10^{17}$	—	1.00[a]
	H_2 773 K, O_2 673 K, H_2 473 K	$0.6_5 \times 10^{19}$	0.38	0.35
C_1	H_2 473 K	0.3×10^{19}	0.96	1.00
	H_2 773 K	$<10^{17}$	—	1.00[a]
C_2	H_2 473 K	0.7×10^{19}	0.09	0.1
	H_2 773 K	$<10^{17}$	—	—
	H_2 773 K, O_2 673 K, H_2 473 K	1.1×10^{19}	0.14	0.15

[a] No noticeable sintering was observed after reduction at 773 K.

and turnover frequencies at 473 K for the reactions of *n*-butane and neopentane obtained in the temperature range 450–520 K. For comparison the table also contains data obtained on a silica-supported catalyst (taken from Ref. *12*).

Influence of Catalyst Pretreatment on the Reactions of n-Butane and Neopentane

Table 4 lists activation energies, turnover frequencies at 473 K, and selectivities for the reactions of *n*-butane and neopentane

TABLE 3

Reaction Data after Reduction at <520 K

Hydrocarbon	Catalyst	Product distribution[a]					E_a (kJ mol^{-1})	N_{473} (molecules s^{-1} Ir$_{(s)}^{-1}$)
		Me	Et	Pr	iso-B	iso-P		
n-Butane	A_1	9.2	72.3	18.5	—	—	169	1.4×10^{-2}
	B_1	6.9	79.6	13.6	—	—	166	2.2×10^{-2}
	C_1	7.0	79.6	13.4	—	—	169	2.0×10^{-2}
	A_2	15.2	53.1	31.5	—	—	140	6.4×10^{-2}
	C_2	19.5	43.5	37.0	—	—	137	16.8×10^{-2}
	1.5% Ir/SiO_2[b]	13.4	61.0	25.6	—	—	170	2.6×10^{-2}
Neopentane	A_1	22.5	15.7	7.5	54.3	—	220	1×10^{-4}
	B_1	16.2	22.5	7.1	54.2	—	215	0.68×10^{-4}
	C_1	16.3	22.8	6.7	54.2	—	220	0.85×10^{-4}
	A_2	26.7	4.5	4.4	62.1	2.3	191	35×10^{-4}
	C_2	27.8	1.6	3.0	64.2	3.4	190	95×10^{-4}
	1.5% Ir/SiO_2[b]	30.1	8.5	3.6	57.8	—	239	0.35×10^{-4}

[a] Product distributions are expressed in percentage of parent converted to indicated product.

[b] Data taken from Ref. (*12*).

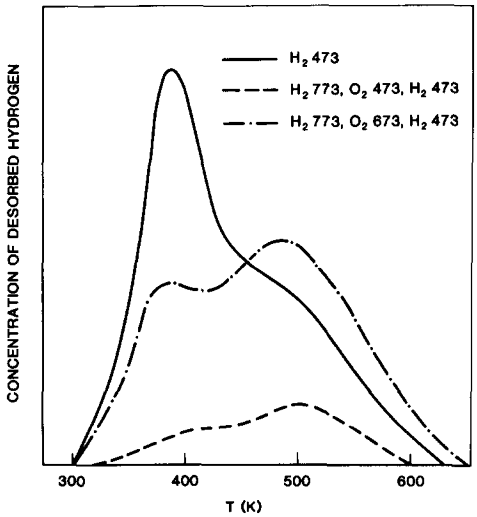

FIG. 2. TPD profiles of hydrogen from catalyst A_2 pretreated at indicated conditions.

as a function of catalyst pretreatment. The selectivities S_2 and S_1 are defined, respectively, as the ethane fraction among the products for the reaction of *n*-butane and the methane/ethane ratio for the reaction of neopentane.

After high-temperature reduction (773 K) all catalysts except C_2 recover activity with increasing time on stream (Fig. 3) and the calculation of activation energies is virtually impossible for both reactions. After about 30 hr on stream a 10- to 100-fold higher activity was measured compared to the value obtained immediately after high-temperature reduction. The slow decrease in activity with increasing time on stream observed on catalyst C_2 can probably be attributed to poisoning by coke deposition. Regeneration treatment at 473 K caused a complete restoration of activities and selectivities for the catalysts A_1, B_1, C_1. However, only partial reactivation is obtained on catalysts A_2 and C_2. Treatment in oxygen at 673 K results in a change of the reaction pattern (selectivities, activation energies, and activities) for all catalysts. Figures 4 and 5 demonstrate the influence of catalyst pretreatment on the reaction selectivity: central bond fission of *n*-butane (*n*-B), methane/ethane ratios from neopentane (neo-P) conversion, and the ratios n_{473}(*n*-B)/N_{473}(neo-P).

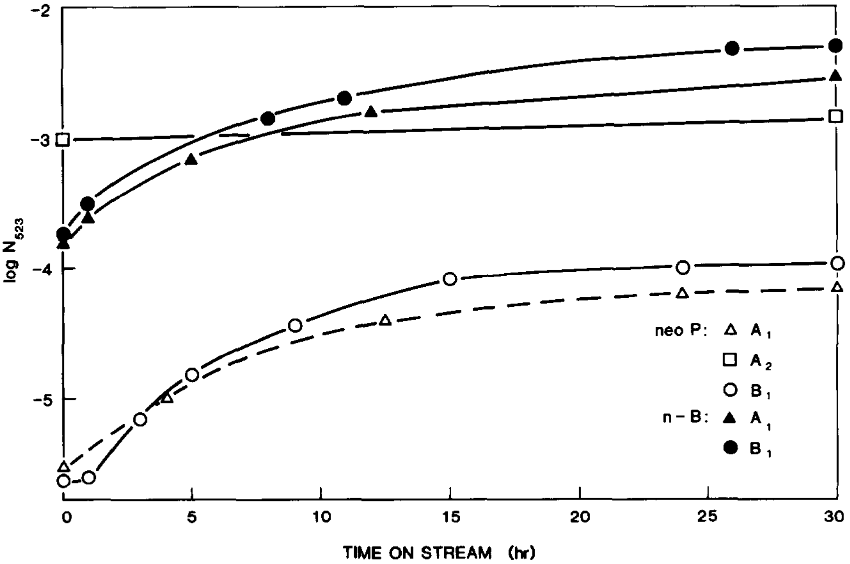

FIG. 3. Changes in activity with time on stream for *n*-butane (full symbols) and neopentane (open symbols) conversions on catalysts A_1, A_2, and B_1 in the SMSI state.

TABLE 4

Reaction Data: Influence of Catalyst Treatment

Catalysts	Pretreatment	*n*-Butane			Neopentane		
		S_2[a]	E_a[b]	N_{473}[c]	S_1[d]	E_a[b]	N_{473}[c]
A_1	H_2 473 K	0.72	169	1.4×10^{-2}	1.5	220	1.0×10^{-4}
	H_2 773 K—initial		NM[e]	$<10^{-6}$		NM	$<10^{-7}$
	H_2 773 K—30 hr on stream	0.56	NM	1.2×10^{-4}	4.2	NM	1.3×10^{-6}
	H_2 773 K, O_2 473 K, H_2 473 K	0.76	170	1.2×10^{-2}	1.6	215	4.8×10^{-5}
	H_2 773 K, O_2 673 K, H_2 473 K	0.65	160	3.5×10^{-2}	3.5	195	6.0×10^{-4}
B_1	H_2 473 K	0.80	167	2.2×10^{-2}	0.8	215	6.8×10^{-5}
	H_2 773 K—initial		NM	$<10^{-6}$		NM	$<10^{-7}$
	H_2 773 K—30 hr on stream	0.50	NM	2.0×10^{-4}	5.6	NM	1.0×10^{-6}
	H_2 773 K, O_2 473 K, H_2 473 K	0.80	170	2.1×10^{-2}	0.8	225	3.7×10^{-5}
	H_2 773 K, O_2 673 K, H_2 473 K	0.60	155	4.5×10^{-2}	5.0	195	9.0×10^{-4}
C_1	H_2 473 K	0.78	169	2.0×10^{-2}	0.7	220	4.2×10^{-5}
	H_2 773 K—30 hr on stream	0.50	NM	1.0×10^{-4}	5.5	NM	7.5×10^{-7}
	H_2 773 K, O_2 473 K, H_2 473 K	0.79	175	2.0×10^{-2}	1.0	215	2.4×10^{-5}
A_2	H_2 473 K	0.53	140	6.4×10^{-2}	5.9	190	3.1×10^{-3}
	H_2 773 K—initial	0.50	NM	4.0×10^{-4}	5.0	NM	3.7×10^{-5}
	H_2 773 K—30 hr on stream	0.49	NM	4.5×10^{-4}	4.0	NM	4.2×10^{-5}
	H_2 773 K, O_2 473 K, H_2 473 K	0.69	160	1.1×10^{-2}	1.2	230	7.6×10^{-5}
	H_2 773 K, O_2 673 K, H_2 473 K	0.58	153	3.6×10^{-2}	5.0	195	9.0×10^{-4}
C_2	H_2 473 K	0.44	137	1.7×10^{-1}	20.0	191	9.5×10^{-3}
	H_2 773 K—initial	0.50	NM	4.0×10^{-3}	21.0	NM	2.2×10^{-4}
	H_2 773 K—30 hr on stream	0.50	NM	3.2×10^{-3}	20.0	NM	1.6×10^{-4}
	H_2 773 K, O_2 473 K, H_2 473 K	0.56	150	1.6×10^{-2}	12.0	193	6.5×10^{-4}
	H_2 773 K, O_2 673 K, H_2 473 K	0.55	151	3.8×10^{-2}	14.0	191	8.6×10^{-4}

[a] S_2 ratio (ethane/total products).

[b] Activation energy in kJ mol^{-1}.

[c] N_{473} molecules s^{-1} $Ir_{(s)}^{-1}$—calculated assuming constant iridium metal surface for treatments 1 to 4.

[d] S_1 ratio (methane/ethane).

[e] Activation energies could not be measured (NM) because of unstable activities.

DISCUSSION

Adsorption and Temperature-Programmed-Desorption (TPD) of Hydrogen

For the fresh catalysts reduced at $T_R \leq 520$ K dispersion values ($D = Ir_{(s)}/Ir_{(total)}$) calculated from monolayer hydrogen uptake (estimated by back-extrapolation to zero pressure from the linear part of the adsorption isotherm) agree closely with those estimated from particle size distributions obtained by TEM. This observation is common for iridium irrespective of the support material. However, if the catalysts are reduced at higher temperatures, significantly lower hydrogen uptakes are measured and, although sintering of the particles could not be substantiated by TEM, the catalysts were unable to adsorb hydrogen after reduction at $T_R = 773$ K. These results are in agreement with the earlier findings by Tauster and Fung (*7*) that metals supported on TiO_2, Nb_2O_3, Ta_2O_5, and V_2O_5 lose their ability to adsorb hydrogen or carbon monoxide after high-temperature reduction. The phenomenon has been explained in terms of a strong metal–support interaction (SMSI) caused by the reduction of Ti^{4+} to Ti^{3+} and electron transfer

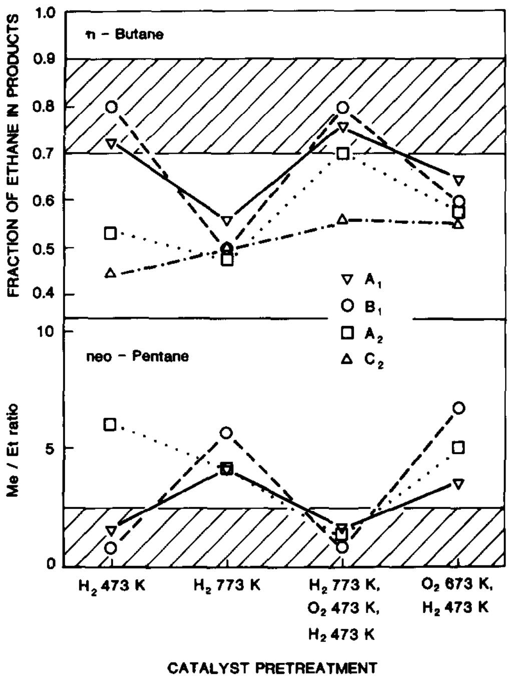

FIG. 4. Selectivities S_1 and S_2 as function of catalyst pretreatment: S_1 (neopentane hydrogenolysis) = ratio: methane/ethane; S_2 (*n*-butane hydrogenolysis) = fraction: ethane/total products. Reaction conditions: T_R = 473 K, $\chi_{HC} = 0.05$. Shaded areas define selectivities for Ir/SiO_2 (Ref. *12*).

from Ti^{3+} to the metal resulting in "electron-rich" metal clusters. If we adopt the concept of donor and acceptor reactions proposed by Schwab (*5*) and classify the adsorption of H_2 and CO as donor interactions (electron donation from adsorbing molecule to the metal cluster) it seems plausible that such interactions would be suppressed on electron-rich metal particles.

Temperature-programmed reduction profiles of our titania-supported noble metals exhibited two distinct reduction regions, one at <500 K which was attributed to the reduction of the impregnated metal compound and a second one starting at 550 K and reaching a maximum at 700 K which has been shown to originate from the reduction of Ti^{4+} to Ti^{3+} by spillover hydrogen atoms from the metal (*10*). ESCA experiments on such catalysts (*10*) proved the existence of "electron-rich" metal clusters after treatment in hydrogen at 800 K, and we are confident that the inability of our iridium/titania catalyst to adsorb hydrogen after high-temperature reduction has to be attributed to strong metal–support interactions of the type proposed by Tauster *et al.* (*6*). Oxygen treatment at 673 K was claimed to restore the intrinsic adsorption characteristic of iridium (*6*). If we treated our SMSI catalysts in 1% oxygen in helium at 673 K for 2 hr sintering was observed with highly dispersed catalysts and hydrogen uptake values were down by factors of two to three; with the catalysts A_2 and C_2 (particle size 3.5 nm and larger), however, some degree of redispersion is observed.

Temperature-programmed desorption (TPD) of hydrogen measured on catalyst A_1 (representing a highly dispersed catalyst) and A_2 (catalyst of lower dispersion) is expected to yield more detailed information about the changes in the nature of the catalysts. A single TPD profile with a maximum

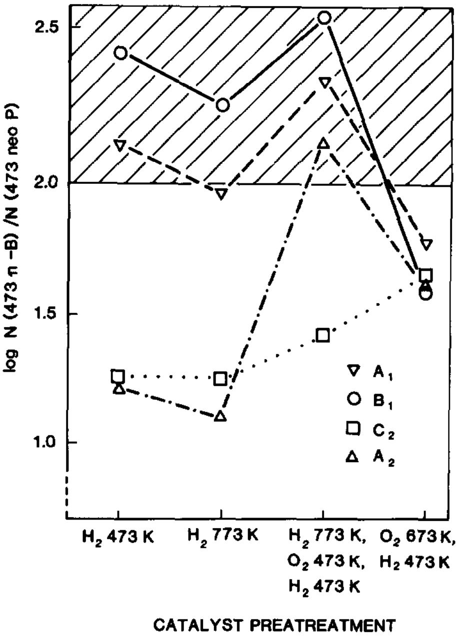

FIG. 5. Variation of ratio: C_2-unit hydrogenolysis to iso-unit hydrogenolysis as a function of catalyst pretreatment. Reaction conditions: T_R = 473 K, χ_{HC} = 0.05. Shaded areas define behavior of Ir/SiO_2 (Ref. *12*).

at 500 K was obtained from the highly dispersed catalyst after reduction at 473 K and adsorption of hydrogen at 289 K. Very similar profiles have already been reported for highly dispersed iridium on silica and alumina (*12*).

For catalyst A_2 with a mean particle size of 3.5 nm the main desorption maximum appeared at 390 K. The shoulder at 500 K is most likely caused by the presence in the catalyst of a significant proportion of very small iridium particles as seen on electron micrographs. A particle size dependence of the hydrogen desorption profile was observed previously with silica-supported iridium (*12*), but the profiles generally extended to fairly high temperatures. The narrower profile observed with A_2 seems to indicate the presence of more uniform adsorption sites on the surface of larger metal particles supported on titania.

An increase in reduction temperature (T_R) of catalyst A_1 caused the TPD profile to shrink in a uniform manner (Fig. 1); at $T_R = 573$ K the area under the desorption peak had fallen by 20%, at $T_R = 673$ K by 90%, and at $T_R = 773$ K no appreciable amounts of hydrogen were desorbed from the catalysts. Subsequent exposure to a stream of 1% oxygen in helium at a temperature as low as 473 K was able to restore completely the TPD profile obtained prior to high-temperature hydrogen treatment of the catalyst.

Negligible amounts of hydrogen were desorbed from catalyst A_2 ($\bar{d}_{Ir} = 3.5$ nm) after high-temperature reduction ($T_R = 773$ K), but in contrast with the behavior of A_1 after subsequent oxidation at 473 K only about 20% of the initial TPD profile is restored. Furthermore, the profile maximum had shifted to 500 K. The results suggest that the SMSI state has been largely destroyed for the very small iridium particles, but not for the larger ones. Treatment in 1% oxygen in helium at 673 K followed by reduction at 473 K restored the ability of A_2 to adsorb hydrogen, but the TPD profile which differs from the initial profile (after reduction at 520 K) by showing a main desorption maximum at 500 K suggests a change in particle morphology. Already in a recent study on the oxidation behavior of silica-supported iridium catalysts at elevated temperatures (*14*) we reported changes of the catalyst structure by treatment in oxygen at temperatures above 573 K which were caused by the formation, evaporation, and redeposition of volatile IrO_2. Bearing in mind those results, it is not unexpected that similar changes are obtained on titania-supported catalysts. We are, at present, carrying out a more detailed study of the influence of the method of preparation and subsequent pretreatment on the structure of titania-supported noble metal catalysts.

Reactions of n-Butane and Neopentane

Catalysts reduced at $T < 520$ K. Two distinct reaction mechanisms for hydrocarbon conversions already have been elucidated for iridium supported on silica or alumina (*12, 13*): a reaction via the *C_2-unit mode* characterized by an activation energy of about 170 kJ mol^{-1} and a turnover frequency at 473 K in the range $1–2.5 \times 10^{-2}$ molecules s^{-1} Ir_s^{-1}, and a reaction via the *iso-unit mode* with an activation energy in excess of 220 kJ mol^{-1} and turnover-frequencies at 473 K below 10^{-4} molecules s^{-1} Ir_s^{-1}. The first of these mechanisms is responsible for the fission of primary–primary, primary–secondary, and secondary–secondary carbon bonds, whereas fission of bonds involving tertiary or quaternary carbon atoms can only proceed via the iso-unit route. C_2-unit hydrogenolysis is intrinsically the more facile reaction and proceeds exclusively even if the structure of the reacting molecule would allow both reaction types to occur, e.g., neopentane and methane are the sole products from the hydrogenolysis of neohexane.

Comparing the results obtained on highly dispersed iridium on titania with the earlier established reaction behavior on silica-supported iridium, a remarkable agreement is noticeable. Activation energies and turnover frequencies measured on the catalysts A_1, B_1, and C_1 are very similar to reaction data reported for Ir/SiO_2 (*12*), and it is reasonable to assume that the hydrocarbon reactions proceed via the same mechanism for iridium on either support. On the other hand, a significant difference does exist if the behavior of less highly dispersed iridium on titania and silica is compared. On silica-supported catalysts both reactions are independent of particle size whereas for Ir/TiO_2 a strong particle size dependence is observed. On the catalysts A_2 ($\bar{d}_{Ir} \simeq 3.5$ nm) and C_2 ($\bar{d}_{Ir} \simeq 10.0$ nm) markedly lower activation energies (around 140 and 190 kJ mol^{-1} for the reactions of *n*-butane and neopentane, respectively) are observed. Turnover frequencies of 6.4×10^{-2} molecules s^{-1} Ir_s^{-1} (threefold increase compared to A_1) and 17.0×10^{-2} molecules s^{-1} Ir_s^{-1} (eightfold increase compared to C_1) are obtained for the conversion of *n*-butane at 473 K. For the neopentane reaction an even more pronounced increase in activity is observed with turnover frequencies 30 to 100 times larger than obtained on the highly dispersed catalysts. Reactions via the iso-unit mode seem to be more affected by structural changes of the catalysts than reactions via the C_2-unit mode, and the strong preference for C_2-unit hydrogenolysis, observed with silica-supported iridium catalysts irrespective of particle size, diminishes on Ir/TiO_2 catalysts with decreasing dispersions. The ratio $N_{473}(n\text{-B})/N_{473}(\text{neo-P})$ proves to be a useful measure for changes in catalyst structure (Fig. 5). The particle size effects are demonstrated in Fig. 6, which for comparison includes data obtained on silica-supported catalysts.

The product distributions obtained in the conversion of *n*-butane and neopentane on titania-supported iridium are similar to the ones observed on silica- and alumina-supported iridium catalysts. The typical reaction pattern of highly dispersed iridium (preferential central bond splitting of *n*-butane, high ethane content of neopentane hydrogenolysis products, and negligible isomerization) was obtained irrespective of support, and silica- as well as titania-supported iridium catalysts of lower dispersions exhibited more nonselective bond splitting of *n*-butane and some isomerization of neopentane.

The results imply that, although it was not apparent from reaction data on silica- or alumina-supported iridium, hydrogenolysis via the "C_2-unit" mode and the "iso-unit"

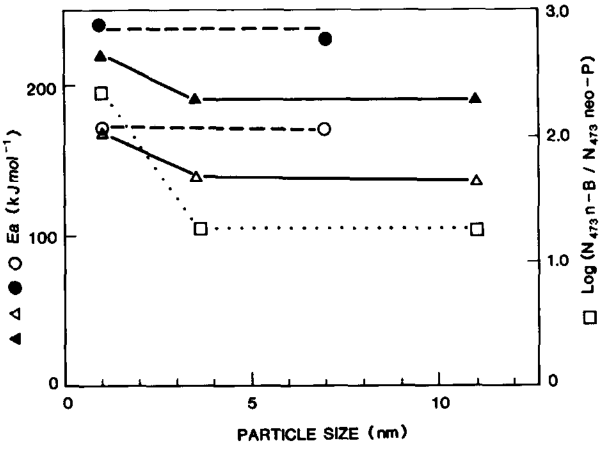

FIG. 6. Variation of activation energies and the ratio C_2-unit hydrogenolysis to iso-unit hydrogenolysis with $\bar{d}_{Ir}$ on catalysts reduced at 473 K. Neopentane: ▲, Ir/TiO_2; ●, Ir/SiO_2 (*12*); *n*-butane: △, Ir/TiO_2; ○, Ir/SiO_2 (*12*); □, Ir/TiO_2.

mode can be structure sensitive. Therefore the highly reactive sites present on iridium particles supported on titania have to be of a type not commonly obtained on the surface of iridium clusters supported on silica. The reported results do not allow a definite assessment of the nature of those reaction sites, and to our knowledge hydrocarbon reactions on oriented films have not been studied. Considering the nature of both supports, it seems reasonable to propose the following explanations for the differences in the behavior of the catalytic systems Ir/SiO_2 and Ir/TiO_2.

On silica, which represents an amorphous support with very weak metal–support interaction, spherical or hemispherical iridium particles are expected to form predominantly, exposing mainly close packed surfaces over a wide range of particle sizes. In contrast, titania is a crystalline support and consists of distinctly shaped crystals exposing definite crystallographic planes. Such planes may force iridium particles of sizes 3.0 nm and larger to adopt a morphology quite different from that assumed by iridium particles supported on silica. Further light on this hypothesis should be provided by the results of a detailed study of the structure of iridium clusters on titania currently in progress in this laboratory. A "chemoepitaxial" effect has been reported earlier by Dalmai-Imelik *et al.* (*1*) for the system nickel antigorite, where depending on the reduction conditions the nickel platelets produced, exposed mainly (111) or (110) surfaces.

Catalysts reduced at 773 K. High-temperature reduction induced the SMSI state in titania-supported iridium catalysts. The interaction is characterized by electron transfer from the reduced support surface to the metal, thus giving rise to "electron-rich" metal particles and a strong suppression of donor interactions of adsorbants or reactants with the metal surface. It has been shown that catalysts in the SMSI state are unable to adsorb hydrogen, and since hydrocarbon reactions can also be classified as donor interactions, significant losses in activity should occur.

Indeed, the initial activities on highly dispersed iridium on titania catalysts decreased by factors of 10^3 to 10^4 after catalyst pretreatment in hydrogen at 773 K for 15 hr. However, the catalysts slowly regained activity with increasing time on stream (Fig. 3) which made it impossible to measure kinetic reaction data. Such behavior has not been reported before. However, Tauster and Fung (*7*) have shown that water and/or oxygen are able to destroy the SMSI state. But a careful examination of the feed by mass spectroscopy did not substantiate the presence of either of these substances, and we are forced to the conclusion that the reaction itself is able to break the metal–support interaction. Since it is very unlikely that saturated hydrocarbons in the feed would be able to interact strongly with Ti^{3+} centers, we suggest that the active species are unsaturated fragments spilled over to the support from the metal particles. To test this hypothesis we induced the SMSI state in catalyst A_1, reacted *n*-butane at 520 K, measured the activity, interrupted the reaction, injected a pulse of butene, and started the reaction again (Fig. 7). Indeed, a significantly higher activity is measured after each pulse.

Over a period of 30 hr on stream a 20- to 100-fold activity gain is obtained. The "equilibrium activity" is, however, still lower than that measured on the catalysts prior to high-temperature reduction by a factor of 10^2. On A_2 and C_2 (catalysts of lower dispersions) high-temperature hydrogen treatment results in a 100-fold decrease in activity, but in contrast to the highly dispersed iridium–titania catalysts they do not regain activity with increasing time on stream.

Changed product distributions are obtained for both reactions on catalysts in the SMSI state. This is especially apparent with highly dispersed iridium, which seems to have lost the preference for central bond splitting in *n*-butane and the ethane fraction

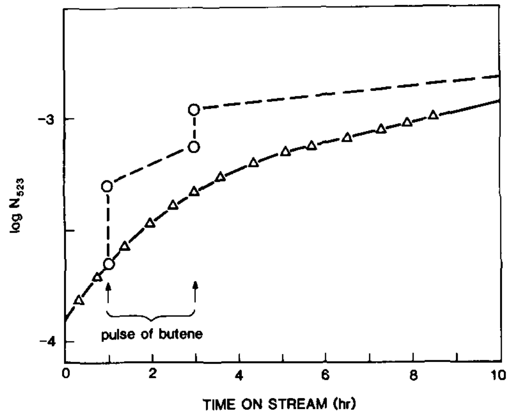

FIG. 7. Activity variation for n-butane hydrogenolysis on catalyst A_1 in the SMSI state: influence of butene pulses. Reaction conditions: $T_R = 523$ K, $\chi_{HC} = 0.05$.

of the neopentane products is markedly lower (Fig. 4). Whether these selectivity changes are solely or partly caused by a change in metal particle morphology due to high-temperature reduction treatment, e.g., formation of "pillbox" structures as reported by Baker *et al.* (*11*) is difficult to assess. Such changes in our system could only be established with certainty by *in situ* electron microscopy.

The small increase in the proportion of isomerization products from the reaction of neopentane may be attributed to the reduction in the availability of adsorbed hydrogen, as already suggested for reactions over iridium–gold catalysts (*13*).

Effect of oxidation on the SMSI state. Oxidation at 473 K followed by reduction at the same temperature destroys the SMSI state in the case of the highly dispersed iridium catalysts, A_1, B_1, C_1, as evidenced by the adsorption properties (Fig. 1) and reaction data (activities and selectivities) which are practically identical to the data measured on the catalysts in the non-SMSI state. The same treatment, however, did not appear to be very effective in breaking the metal–support interaction of the larger particles ($\bar{d}_{Ir} > 3.5$ nm) which predominate in catalysts A_2 and C_2. The greater activity gain shown by A_2 (compared to C_2) must reflect the contribution of the significant proportion of very small iridium particles observed to be present in the catalyst. These particles are preferentially activated and as a consequence the observed reaction behavior is characterized by central bond splitting in n-butane hydrogenolysis, higher activation energies for the reactions of n-butane as well as neopentane, and high selectivity toward C_2-unit hydrogenolysis, which is the typical reaction pattern obtained on highly dispersed iridium (Fig. 4). Furthermore, oxidation at 473 K was able to restore only 5 to 10% of the initial catalyst activity in the case of catalyst C_2 where very small particles are largely absent.

It is by no means obvious why treatment in oxygen at 473 K should be sufficient to destroy the SMSI state in highly dispersed iridium catalysts ($\bar{d}_{Ir} < 2.0$ nm) but not in catalysts of lower dispersions ($\bar{d}_{Ir} > 3.5$ nm). However, further studies on the structural changes which titania-supported metal catalysts of various dispersions undergo as a function of catalyst pretreatment should lead to a better understanding of this phenomenon.

According to Tauster *et al.* (*6*) oxidation treatment at 673 K, followed by low-temperature reduction (473 K) restores the adsorption capacity and reactivity of titania-supported catalysts, and indeed the hydrogen uptake on catalysts A_2 and C_2 is even slightly higher than that measured on the catalysts before high-temperature hydrogen treatment. In contrast, highly dispersed catalysts seem to lose some metal surface area. A comparison of the reaction pattern (Table 4) obtained on all catalysts before inducing the SMSI state and after oxidation of SMSI catalysts at 673 K clearly reveals considerable differences, and suggests that all catalysts have undergone significant structural changes. This is not surprising as we have already demonstrated that under these oxidation conditions iridium supported on silica or alumina transforms into IrO_2 (*14*).

Nevertheless, there exists a distinct difference between silica- and titania-supported catalysts in terms of the structure and size of iridium particles produced by reduction of the oxidized catalysts. IrO_2 was shown to form large lath or boomerang-shaped crystals on silica or alumina (*14*), whereas on titania a thin film of IrO_2 seems to cover the rutile or anatase crystals. On reduction the IrO_2 on silica transforms into large agglomerates of crystallites with a much reduced surface-to-volume ratio. On the other hand, the IrO_2 "film" on titania is converted on reduction to nests of unattached small iridium particles (see Fig. 8).

CONCLUSIONS

(1) The reaction data measured for *n*-butane (representative of a molecule reacting via C_2-unit hydrogenolysis) and neopentane (reacting via iso-unit hydrogenolysis) on highly dispersed iridium/titania catalysts reduced at $T_R < 520$ K are in good agreement with the reaction pattern reported for highly dispersed silica-supported iridium catalysts.

(2) Whereas on Ir/SiO_2 or Ir/Al_2O_3 both reactions seem to be independent of metal particle size, a strong particle size dependence was observed with the Ir/TiO_2 system. Larger iridium particles supported on titania seem to expose highly reactive sites for hydrogenolysis of *n*-butane and neopentane.

(3) High-temperature (773 K) reduction in hydrogen resulted in a strong metal–support interaction (SMSI) of the type proposed by Tauster *et al.* (*6*) and Horsley (*8*). Hydrogen adsorption and hydrocarbon reactions are strongly suppressed on such catalysts. Changes in the selectivity of SMSI catalysts may be attributed to additional structural changes of the metal particles due to the strong interaction with the support, e.g., formation of "pillbox" structures as reported for Pt/TiO_2 (*11*), but further work has to be carried out to elucidate evidence for such structures.

(4) The SMSI state can be destroyed by oxidation and subsequent reduction at 473 K in the case of highly dispersed catalysts and the consequent reaction pattern is the same as that observed on the catalysts prior to the high-temperature hydrogen treatment. For iridium–titania catalysts of lower dispersions, higher oxidation temperatures (673 K) are necessary to break SMSI. However, bulk IrO_2 forms at oxidation tempera-

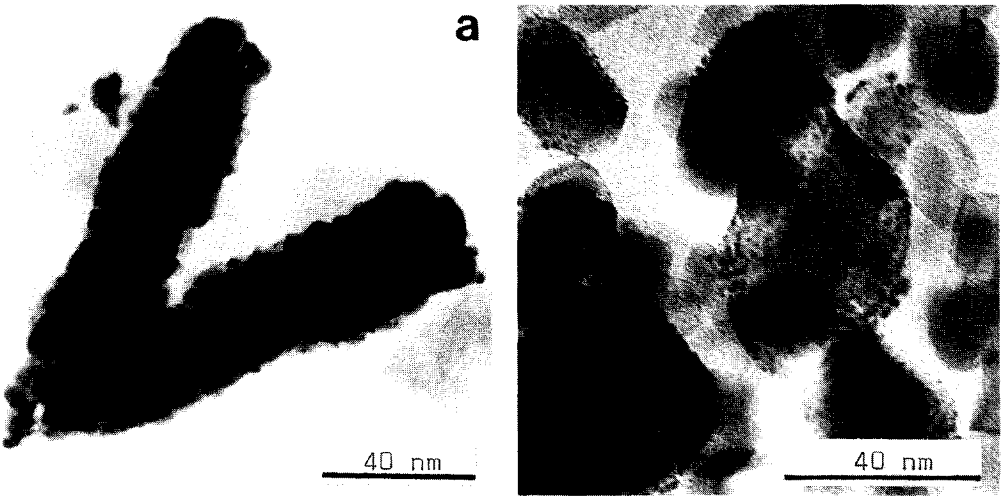

FIG. 8. Electron micrographs of iridium on silica (a) and iridium on titania (b) after oxidation in 1% oxygen in helium at 820 K followed by reduction at 570 K.

tures above 573 K causing irreversible structural changes in all catalysts.

ACKNOWLEDGMENTS

The author is grateful to Mr. H. Jaeger for taking the electron micrographs, Mr. A. E. Hughes for the XPS measurements, and wishes to thank Dr. J. R. Anderson for valuable discussions in preparing this manuscript and Mr. J. Spink for critical reading of the manuscript.

REFERENCES

1. Dalmai-Imelik, G., Leclercq, C., and Maubert-Muguet, A., *J. Solid State Chem.* **16,** 129 (1976).
2. Dalla Betta, R. A., and Boudart, M., *in* "Proceedings, 5th International Congress on Catalysis" (J. W. Hightower, Ed.), p. 139. North-Holland, Amsterdam, 1973.
3. Foger, K., and Anderson, J. R., *J. Catal.* **54,** 318 (1978).
4. Gallezot, P., Alarcon-Diaz, A., Dalmon, J. A., Renouprez, A. J., and Imelik, B., *J. Catal.* **39,** 334 (1975).
5. Schwab, G. M., *Adv. Catal.* **27,** 1 (1978).
6. Tauster, S. J., Fung, S. C., and Garten, R. L., *J. Amer. Chem. Soc.* **100,** 170 (1978).
7. Tauster, S. J., and Fung, S. C., *J. Catal.* **55,** 29 (1978).
8. Horsley, J. A., *J. Amer. Chem. Soc.* **101,** 2870 (1979).
9. Fung, S. C., *J. Catal.* **76,** 225 (1982).
10. Sexton, B. A., Hughes, A. E., and Foger, K., *J. Catal.* **77,** 85 (1982).
11. Baker, R. T. K., Prestridge, E. B., and Garten, R. L., *J. Catal.* **56,** 390 (1979).
12. Foger, K., and Anderson, J. R., *J. Catal.* **59,** 325 (1979).
13. Foger, K., and Anderson, J. R., *J. Catal.* **64,** 448 (1980).
14. Foger, K., and Jaeger, H., *J. Catal.* **70,** 53 (1981).